

Study the high pressure effect on compressibility factors of high CO₂ content natural gas

Huang Liu^{a,*}, Zhengkun Tian^a, Ping Guo^a, Qian Li^b, Zhouhua Wang^a, Wenjuan Wang^c, Jianfen Du^a, Yunfan Wen^a

^a State Key Lab of Oil and Gas Reservoir Geology and Exploitation (Southwest Petroleum University), Rd.8, Xindu District, Chengdu City, Sichuan Province, 610500, PR China

^b Research Institute of Exploration and Development, PetroChina Southwest Oil & Gas Field Company, Chengdu, 610041, China

^c CNOOC China Limited, Zhanjiang Branch, Zhanjiang, Guangdong, 524057, China



ARTICLE INFO

Keywords:

Natural gas
Compressibility factor
High CO₂ concentration
Thermodynamic model

ABSTRACT

The aim of this work was to study the effect of high pressure on the compressibility factors of natural gas with a high CO₂ content. The obtained research results are important for reservoir and ground engineers. The compressibility factors (Z-factors) of three real natural gas samples (called sample 1, sample 2, and sample 3), and five synthetic gases formed by injecting different amounts of CO₂ (10 mol%, 30 mol%, 50 mol%, 75 mol%, 90 mol%) into sample 2 (called sample 4–8) were determined at their reservoir temperatures. The real reservoir temperature and pressure for sample 3 reached 463.15 K and 96 MPa, respectively. The experimental results showed that the Z-factors of all eight gas samples first decreased with decreasing pressure. Then, after the pressure decreased to some degree, the Z-factors began to increase with a further decrease in pressure. Ultra-high temperature and pressure reservoir conditions made the Z-factors of sample 3 much higher than those of sample 1 and sample 2. The injection of CO₂ substantially decreased the Z-factors of sample 2. When 90 mol% CO₂ was injected, the decrease of the Z-factor at its reservoir pressure reached 24.05%. A thermodynamic model based on an equation of state was further developed to describe the Z-factors of the natural gas samples containing CO₂, in which a new correlation for calculating the *m* parameter in the *a*(T) function of the Soave–Redlich–Kwong equation of state was proposed. Meanwhile, new interaction correlations between the CO₂ and CH₄ and the other gas components were also constructed. The calculated Z-factors were in good agreement with the experimental data (116 points) obtained in this work and that (418 points) reported in the literature, with an absolute average deviation of within 1%.

Credit author statement

Huang Liu: Put forward the project concept and completed the last draft of the paper. Zhengkun Tian: Performed the experiments. Ping Guo: Supervision. Huang Liu and Qian Li: Performed data analysis. Zhouhua Wang: Prepared Figures and Tables. Wenjuan Wang: Sampled the gas samples. Jianfen Du: Performed simulation. Yunfan Wen: Wrote the first draft of the paper.

1. Introduction

In contrast to notable swing in the price of crude oil over the past several years, both the global output and price of natural gas have shown

relatively steady increases. Natural gas is a clean and environmentally friendly source of energy (Wang and Economides, 2009). To meet the rapid increase in natural gas consumption, some unconventional natural gas resources such as shale gas (Bowker, 2007) and low/ultra-low permeability gas reservoirs (Zou et al., 2012) have been exploited around the world. In particular, low/ultra-low permeability natural gas production has become an important part of the growth in natural gas production in China (Zeng et al., 2016; Zhang et al., 2018; Yin et al., 2017). For example, the natural gas produced from the low/ultra-low permeability gas reservoirs in the Tarim region has become the main energy source for supporting the development of the Yangtze River Delta economic circle of China. However, although they represent abundant reserves, the low-permeability reservoir cores of these gas reservoirs

* Corresponding author.

E-mail address: liuhuangswpu@sina.com (H. Liu).

have limited gas flow, which usually results in a much lower gas recovery than that found for normal natural gas reservoirs. Furthermore, when the gas is extracted, the pressure of the gas reservoir gradually decreases, along with the core permeability, as a result of the so-called core stress sensitivity (Dou et al., 2016), which restricts the flow of gas in a low-permeability reservoir. CO₂ flooding is regarded as a potential method for increasing the recovery of low/ultra-low permeability gas reservoirs (Mamora and Seo, 2002). Shi et al. (2017) conducted a laboratory investigation of the feasibility of supercritical CO₂ flooding for a tight gas reservoir and found that a ~12% increase in gas recovery could be obtained through CO₂ flooding. Dria et al. and Pope et al. (Dria et al., 1993) conducted core flow experiments to measure the three-phase gas/oil/brine permeability under CO₂ flooding conditions. The results showed that the relative permeability of each phase depended only on the saturation of that phase instead of on the other two saturations. The possible mechanisms of the CO₂ flooding of a low/ultra-low permeability gas reservoir include replacing the adsorbed gases on the core pore surface, weakening the stress sensitivity of the core by maintaining a relatively high pressure for the reservoir, and sequestering the CO₂.

Although there are many advantages, as previously mentioned, the influence of CO₂ injection on the volumetric property of the natural gas could not be ignored. The most important factor of the volumetric property to be evaluated by engineers in planning the development of a natural gas reservoir is the compressibility factor (Z-factor), which is an important parameter for the basic engineering and performance of technique processes (Sanjari and Nemati Lay, 2012; Kumar, 2004; Kamyab et al., 2010). It is known that the Z-factor of CO₂ is usually somewhat smaller than that of CH₄ under the same conditions, especially at high temperatures and pressures (Katz, 1959). Meanwhile, in addition to CO₂ injection, some high CO₂-containing natural gas resources have also been found around the world. Some of these sources with CO₂ contamination exceeding the tolerance values are located in Germany (Pannonian Basin), Australia (Cooper-Eromanga basin) (Krooss et al., 2002), and Northeastern China (Wei et al., 2009). In short, it is important to understand the volumetric properties of these CO₂-natural gas mixtures.

Experimental measurement is of primary importance to determine the Z-factor value of natural gas. Substantial Z-factor data for natural gases have been obtained and reported in the literature (Hou et al., 1996; Fayazi et al., 2014; Li and Guo, 1991; Sanjan and Lay, 2012). However, in most cases, the CO₂ concentration has been low (<10 mol %). Bian et al. (2012) measured the Z-factor values of some CO₂-natural gas mixtures in a high pressure PVT cell, where the highest CO₂ concentration reached 50.99 mol%. They found that the Z-factor decreased with an increase in the CO₂ content of the natural gas. It should be noted that the temperature range they considered was 263.15–313.15 K, which is somewhat smaller than that of most real natural gas reservoirs. Empirical correlations for calculating the Z-factor of a gas are regarded as simple. On the basis of the Standing and Katz Z-factor chart, Beggs and Brill. (1973) proposed a Z-factor correlation that was a function of the pseudo-reduced pressure and temperature, but this correlation was not suggested for use for a reduced temperature of less than 0.92. After that, many Z-factor correlations associated with a pseudo-reduced pressure and temperature were proposed (Kumar, 2005; Heidaryan et al., 2010; Ehsan et al., 2010; Sanjari and Lay, 2012; Xiao et al., 2012). It should be noted that the accuracy of an empirical correlation usually depends on the quantity of data used to construct it. Compared to empirical correlations, a thermodynamic model based on an equation of state (EOS) is regarded as more reliable. Mohsen-Nia et al. (Mohsen-Nia et al., 1994) used a simple two-constant cubic EOS to calculate the thermodynamic properties and phase behavior of sour natural gases. By modifying the OU/GRI EOS, Li and Guo (1991) calculated the Z-factor values of five natural gas mixtures. Yan et al. (2013) calculated the Z-factor of a high temperature and pressure natural gas on the basis of the Soave–Redlich–Kwong (SRK) EOS, where a transition function was

introduced to improve the prediction accuracy. In addition, some new calculation methods such as artificial neural network (Sanjari and Nemati Lay, 2012), intelligent (Kamari et al., et al.), and soft computing methods (Fayazi et al., 2014) have also been reported to calculate the Z-factor values of gases. Sanjari et al. and Lay et al. (Sanjari and Nemati Lay, 2012) modeled the compressibility factors of different compositions of natural gas using an artificial neural network based on the back-propagation method, and the proposed method provided more accurate results than the commonly used empirical models and EOSs of Peng–Robinson and the statistical association fluid theory. Fayazi et al. and Arabloo et al. (Fayazi et al., 2014) implemented a new soft computing approach called the least square support vector machine (LSSVM) model optimized using a simulated annealing optimization technique, and the results showed that the developed LSSVM model outperformed all the existing predictive models, with an average absolute relative error of 0.19% and a correlation coefficient of 0.999. It is necessary to further examine these calculation methods to determine their adaptability to natural gas specimens with high CO₂ contents, and under ultra-high reservoir temperature and pressure conditions.

This study first measured the volumetric properties of two natural gas samples collected from real low-permeability natural gas reservoirs in the Ordos basin, and one ultra-high pressure natural gas sample with a high CO₂ content from the South China Sea in China. Then, the influence of the amount of CO₂ injected (10, 30, 50, 75, and 90 mol%) on the Z-factors of one gas sample were systematically investigated. A high-precision thermodynamic model based on the modified SRK EOS was further built to describe the Z-factors of these natural gases.

2. Research methodology

2.1. Experimental apparatus

To determine the Z-factors of samples 1 and 2, a PVT system manufactured by DBR Co., Canada, was used. A schematic diagram of the experimental device is shown in Fig. 1. It mainly included a high-pressure PVT cell and gas sampler, where the maximum working pressure and temperature of the PVT cell were 70 MPa and 423 K, respectively. Its working volume could be adjusted by pushing a piston in the cell with a motor, and the maximum value was 80 ml. An air bath was used to provide high temperature for the system. To clearly observe the experimental phenomenon occurring in the cell, a LG100H luminescence source was fixed to the outside of the cell. The uncertainties of the pressure and temperature measurements were ±0.01 MPa and ±0.1 K, respectively. The change in the system pressure was recorded using a computer.

Because of its ultra-high reservoir pressure, the phase behavior apparatus manufactured by Sanchez Technologies Co. (see Fig. 2), France, was used to determine the Z-factors of sample 3, as described in detail in our previous work (Strvjec and Vera, 1986). The main part of the apparatus was a high-pressure PVT cell, and its maximum working volume, working pressure, and working temperature were 240 mL, 150 MPa, and 473.15 K, respectively.

2.2. Sample preparation

Natural gas specimens (samples 1 and 2) were collected from two low permeability natural gas reservoirs in the Ordos Basin of China, and sample 3 was obtained from an ultra-high temperature and pressure gas reservoir in the South China Sea. The reservoir pressure and temperature for sample 1 were 23.5 MPa and 348.15 K, those for sample 2 were 25 MPa and 358.15 K, and those for sample 3 reached 456.65 K and 96 MPa, respectively. Five additional samples (samples 4–8) were prepared by injecting different amounts of pure CO₂ into sample 2 in the laboratory. The compositions of all these gas samples were analyzed using an HP 6890 gas chromatograph (with an expanded mole fraction uncertainty of $2\text{--}5 \times 10^{-4}$). Each gas sample was measured three times, and

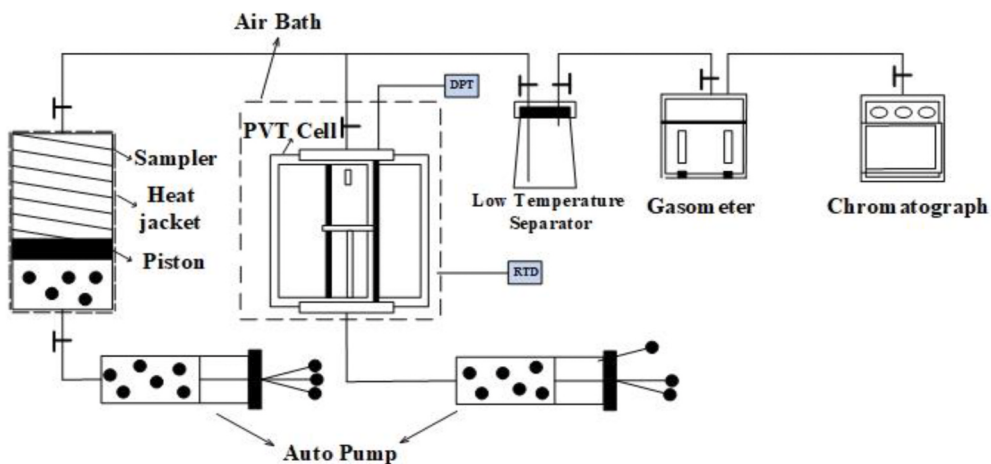


Fig. 1. Schematic diagram of DBR phase behavior experimental apparatus.

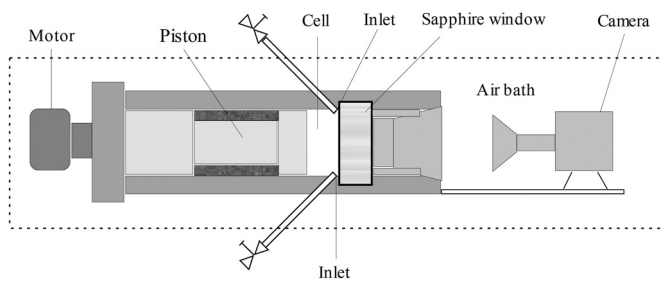


Fig. 2. Schematic diagram of ST phase behavior experimental apparatus.

the average value was used as the composition of the gas mixture. The compositions of these gas samples are listed in Table 1. As can be seen, in addition to CH₄, there were some low-carbon hydrocarbons in both sample 1 and sample 2, and the CO₂ concentration in sample 3 reached 58.35 mol%.

2.3. Research method

The experimental measurements were conducted by transmitting some pre-heated high-pressure feed gas in the sampler into the PVT cell. A constant composition expansion (CCE) test was performed to determine the Z-factor of the gas fluid at its reservoir temperature and different pressures. First, the gas in the PVT cell was subjected to a pressure that was somewhat higher than its reservoir pressure. After that, the pressure (*P*) in the cell was decreased in steps at a constant temperature, and the volume (*V*) of the gas in the cell was obtained by measuring the height of the gas phase (see Fig. S1). It should be noted that when using the ST apparatus, *V* was recorded directly through the connected software. After the pressure in the cell was decreased to the desired low value, all the gas in the PVT cell was discharged to

atmospheric pressure, and the gas volume (*V*₁) was measured through a gas meter (with an accuracy of 1.0 mL). The compressibility factors of the gas fluid at different pressures could then be calculated using the following expression:

$$Z_i = \frac{Z_1 T_1 P_i V_i}{T_i P_1 V_1} \quad (1)$$

where *T*_i and *T*₁ are the experimental temperature and ambient temperature (293.15 K), respectively; *P*_i and *P*₁ are the experimental pressure and atmospheric pressure (0.101325 MPa), respectively; *V*_i and *V*₁ are the fluid volumes at *T*_i and *P*_i, and at *T*₁ and *P*₁, respectively. *Z*_i and *Z*₁ are the compressibility factors of the fluid at *T*_i and *P*_i, and at *T*₁ and *P*₁, respectively, where *Z*₁ was considered equal to 1.0. The detailed calculation processes for *V*_i when using the DBR phase behavior apparatus are presented in the Supporting Information. The *V*_i value of the gas in the ST phase behavior apparatus could be read directly through the connected software.

3. Experimental results

Following the experimental procedures, the *P*-*V*_r curves of sample 1, sample 2, and sample 3 were first obtained (Fig. 3), where *V*_r was the volume ratio between the measured *V* value of the gas fluid in the PVT cell at different pressures with that at the reservoir pressure. The detailed experimental data for determining *V*_r under different pressures are presented in the Supporting Information (Tables S1–S5). As Fig. 3 shows, *V*_r quickly increased with a decrease in the pressure, and the *V*_r value of sample 1 was somewhat smaller than that of sample 2 at the same pressure. This should have been because of the larger quantity of C₂–C₄ hydrocarbons and CO₂ in sample 1 than in sample 2. For sample 3, it can be noted that because of its ultra-high reservoir pressure, the *V*_r value of sample 3 was much higher than those of sample 1 and sample 2. On the basis of Fig. 3 and equation (1), the Z-factors of these three

Table 1
Compositions of gas samples considered in this work.

Components	sample 1	sample 2	sample 3	sample 4 ^a	sample 5 ^a	sample 6 ^a	sample 7 ^a	sample 8 ^a
CH ₄ (mol%)	86.52	97.28	33.74	87.34	68.04	48.62	24.31	9.70
C ₂ H ₆ (mol%)	7.97	1.83	0.69	1.69	1.3	0.95	0.47	0.19
C ₃ H ₈ (mol%)	1.92	0.25	0.11	0.22	0.18	0.13	0.06	0.03
N ₂ (mol%)	1.60	0.64	7.03	0.66	0.51	0.35	0.18	0.07
CO ₂ (mol%)	1.34	—	58.35	10.09	29.97	49.96	74.98	90.01
C ₄ H ₁₀ (mol%)	0.65	—	0.05	—	—	—	—	—
C ₅ H ₁₂ (mol%)	—	—	0.03	—	—	—	—	—

^a Sample 4 was prepared by injecting 10 mol% CO₂ into sample 2; Sample 5 was prepared by injecting 30 mol% CO₂ into sample 2; Sample 6 was prepared by injecting 50 mol% CO₂ into sample 2; Sample 7 was prepared by injecting 75 mol% CO₂ into sample 2; Sample 8 was prepared by injecting 90 mol% CO₂ into sample 2.

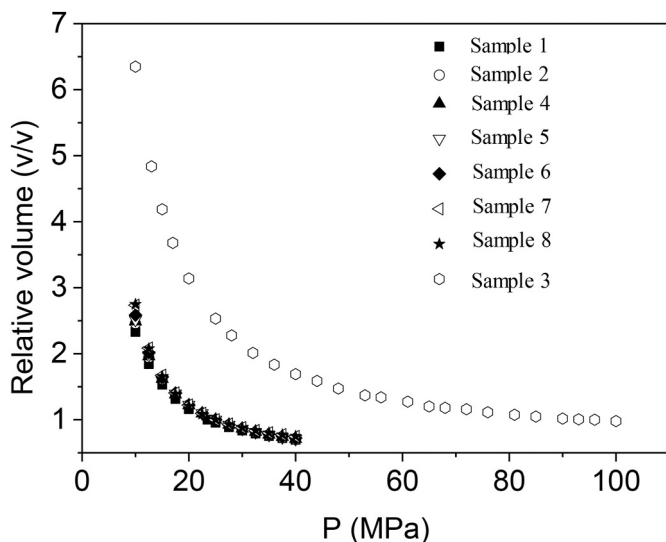


Fig. 3. Changes in P - V_r curves of studied natural gases.

samples were further obtained, and are shown in Fig. 4 and listed in Tables S6 and S7. Unlike the P - V_r curves, for each gas sample, the Z-factors first quickly decreased with a decrease in the pressure, after which the pressure decreased to some degree (around 17.5 MPa for sample 1, around 15 MPa for sample 2, and around 17 MPa for sample 3). The Z-factors then increased with a further decrease in pressure. Corresponding to the P - V_r curves, the higher amounts of C2–C4 hydrocarbons and CO₂ made the Z-factor of sample 1 some smaller than that of sample 2. For sample 3, even though it had the highest CO₂ concentration, because of its ultra-high reservoir temperature and pressure, it showed the highest Z-factors compared to sample 1 and sample 2 at the same pressures.

After that, CCE tests for sample 2 with five different amount of injected CO₂ (10, 30, 50, 75, and 90 mol%) were performed at 358.15 K. The V_r - P curves of these experimental runs are also shown in Fig. 3, on the basis of which the Z-factors of these gases were also calculated (Fig. 4). Evidently, the Z-factors quickly decreased with an increase in the CO₂ concentration in the natural gas. This should have been due to the stronger interaction between the CO₂ and the other gas components compared to that between hydrocarbons, which is in good agreement with the results reported in the literature (Sanjan and Lay, 2012). To further understand the influence of the CO₂ injection on the Z-factors of

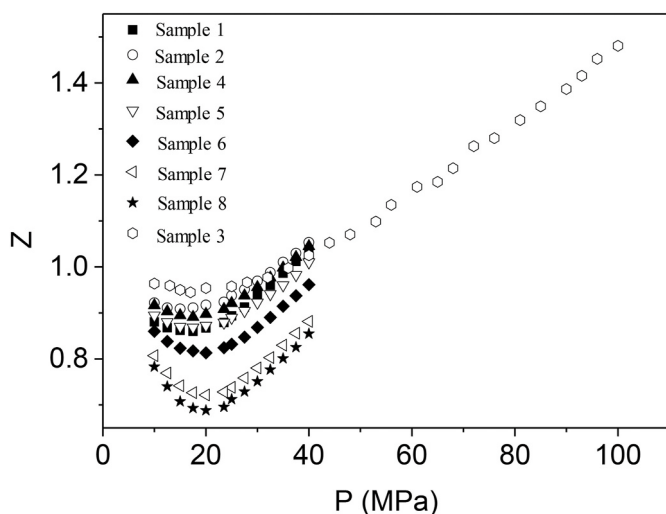


Fig. 4. Z-factors of studied natural gases.

sample 2, the reduction ratio (R) values of the Z-factor of sample 2 at its reservoir pressure (25 MPa) with different amounts of CO₂ injected were calculated:

$$R = \frac{Z_r - Z_{r+CO_2}}{Z_r}, \quad (2)$$

where Z_r is the Z-factor of sample 2 at 25 MPa and 358.15 K; Z_{r+CO_2} is the Z-factor of the CO₂ + sample 2 mixtures at 25 MPa and 358.15 K with different amounts of CO₂ injected. As Fig. 5 shows, the reduction ratio (R) of the Z-factor of sample 2 nearly showed linear growth with an increase in the CO₂ concentration, demonstrating the strong influence of CO₂ injection on the volume property of natural gas.

In short, combining the experimental results mentioned above, it can be concluded that both the reservoir conditions (including the temperature and pressure) and CO₂ concentration had important effects on the Z-factors of the natural gases. An increase in the CO₂ concentration significantly decreased the Z-factors, while increases in the temperature and pressure increased the Z-factors. The influence of the reservoir conditions seemed to be relatively more obvious.

4. Thermodynamic model

Usually the existence of sour gas components such as CO₂ make it harder to predict the Z-factors of natural gases. Several attempts have been made to increase the performance of a thermodynamic model in describing the volumetric properties of natural gases, include tuning the EOS (Huron and Vidal, 1979), establishing new mixing rules (Liu et al., 2019), and applying new binary interaction parameters (k_{ij}) (Strvjejk and Vera, 1986). In this work, a new thermodynamic model was built to describe the Z-factors of natural gases with different CO₂ concentrations and a wide range of reservoir pressures. A correlation to calculate the m parameter in the $a(T)$ function was introduced to improve the description of the volumetric properties of natural gases containing high CO₂ concentration in the SRK EOS.

4.1. Development of model

(1) Original SRK EOS (Soave, 1972):

$$\alpha(T_r), \quad (3)$$

$$\alpha(T_r), \quad (4)$$

$$\alpha(T_r), \quad (5)$$

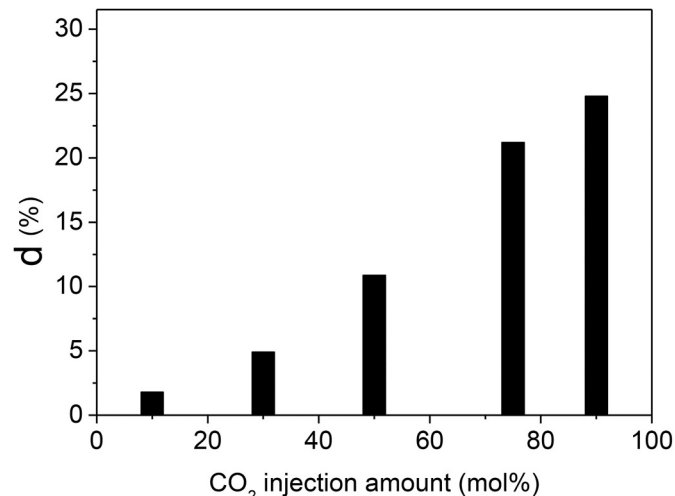


Fig. 5. Reduction ratio of Z-factor of sample 2 with different amounts of injected CO₂ at reservoir pressure (25 MPa).

where p is the system pressure; R is the molar gas constant, which is approximately equal to 8.314472; T is the system temperature; a is the molecular gravitational coefficient; b is the molecular repulsion coefficient; V is the molecular volume; $\alpha(T)$ is a temperature function; T_r is the relative temperature; T_c is the critical temperature; and P_c is the critical pressure.

The value of $\alpha(T_r)$ was calculated using the following expression:

$$\alpha(T_r) = \left(1 + m \left(1 - \sqrt{T_r}\right)\right)^2 \quad (6)$$

A new correlation was developed to calculate parameter m in equation (6), in which the influences of both ω and T_r on m were considered:

$$m = 0.48 + 1.574 \times \omega - 0.176 \times \omega^2 + 4.2529 \times 10^{-2} \times \left(1 + \sqrt{T_r}\right) \times (0.5 - T_r). \quad (7)$$

Van der Waals-type single-fluid mixing rules for EOS parameters a and b were used during the calculation process:

$$a = \sum_i \sum_j x_i x_j (a_i a_j)^{0.5} (1 - k_{ij}) \quad (8)$$

$$b = \sum_{i=1}^n x_i b_i \quad (9)$$

- (2) For the interactions (k_{ij}) between CH_4 and the other components, the interaction parameters were calculated using the following expression:

$$k_{\text{CH}_4-j} = 8.0335 \times 10^{-3} - 0.2063 \times \left(\omega_j^{0.5} - \omega_{\text{CH}_4}^{0.5}\right) \quad (10)$$

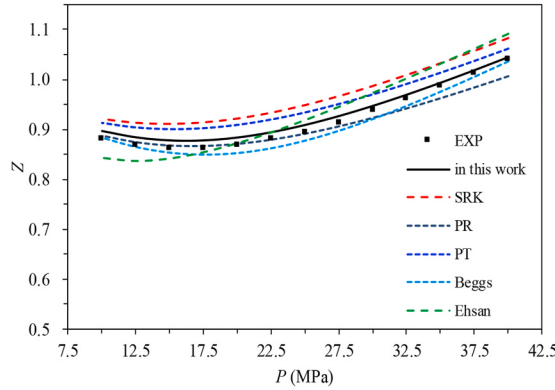
where j refers to components other than methane in the gas sample.

The following correlation was used for the k_{ij} interactions between CO_2 and the other components:

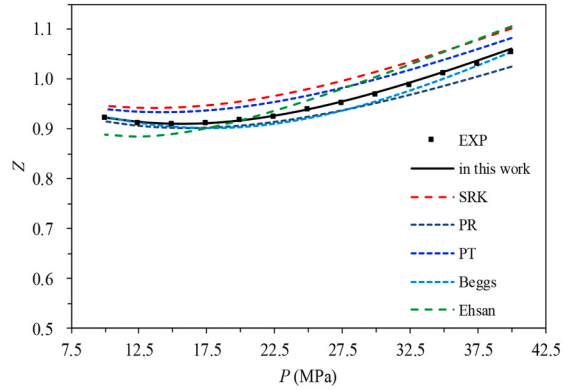
$$k_{\text{CO}_2-j} = 1.18869 \times 10^{-1} + 0.9765 \times \frac{\omega_j}{\omega_{\text{CO}_2}} - 2.0256 \times \left(\frac{\omega_j}{\omega_{\text{CO}_2}}\right)^2 \quad (11)$$

where, in this case, j refers to components other than CO_2 in the gas samples. It should be noted that equation (11) was used to calculate k_{ij} between CO_2 and CH_4 .

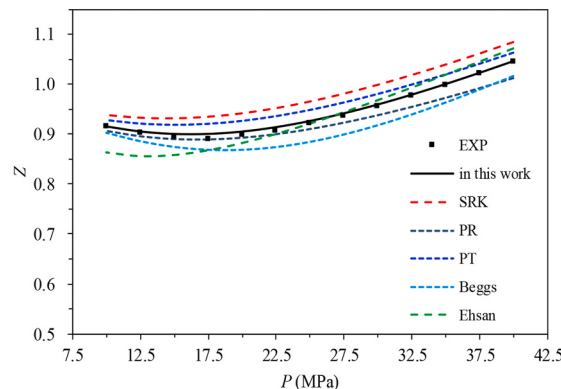
Furthermore, the hydrocarbon–hydrocarbon and N_2 –hydrocarbon binary interaction parameters (k_{ij}) that did not contain CH_4 and CO_2 were considered to be equal to zero. It should be noted that we reported the forms of equations (10) and (11) in previous studies (Strijek and Vera, 1986; Guo et al., 2020). In this work, the coefficients in these two equations and equation (7) were refitted based on the experimental data. In order to increase the application ability of the proposed model, 165 experimental data points reported by Buxton (1965) were also used for the coefficient regression process. These experimental data points had a temperature range of 310–344 K, pressure range of 7.08–48.46 MPa, and CO_2 concentration range in the feed gases of 0–20.16 mol%.



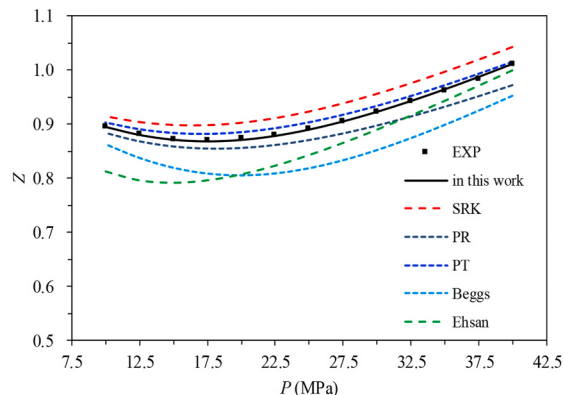
(a)



(b)



(c)



(d)

Fig. 6. Comparisons of experimental Z-factors of gas samples and results calculated using four thermodynamic models (that proposed in this work, SRK EOS, PR EOS, and PT EOS) and four empirical correlations (Beggs (Beggs and Brill., 1973) and Ehsan (Ehsan et al., 2010)): (a) sample 1, (b) sample 2, (c) sample 4, (d) sample 5, (e) sample 6, (f) sample 7, (g) sample 8, and (h) sample 3.

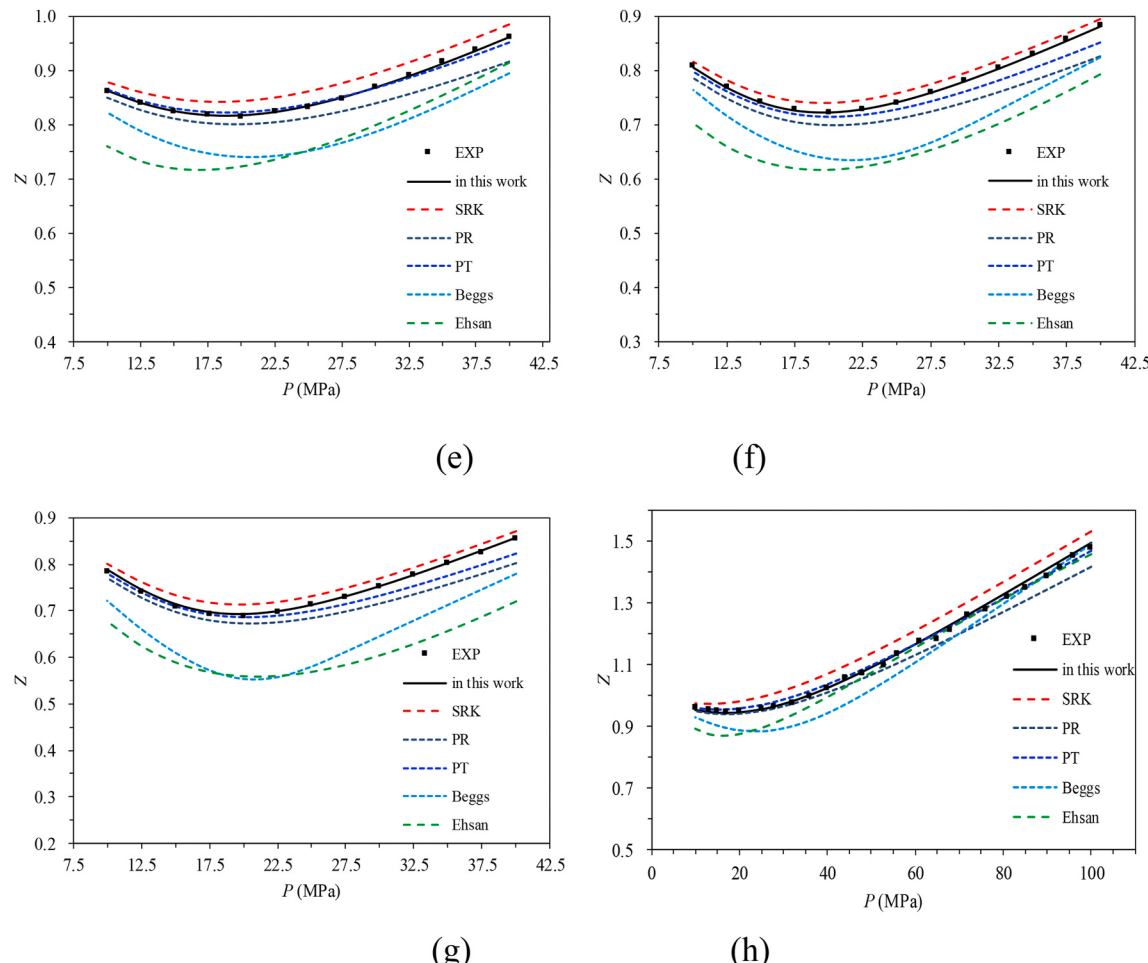


Fig. 6. (continued).

4.2. Modeling results

Fig. 6 compares the calculated and experimental Z-factors of the gas mixtures listed in Table 1. For comparison, the results of Z-factor simulations that used thermodynamic models based on the original SRK (Soave, 1972), PR (Peng and Robinson, 1976), and PT (Patel and Teja, 1982) EOSs and the empirical correlations proposed by Beggs (Beggs and Brill., 1973) and Ehsan (Ehsan et al., 2010) are also presented. It should be noted that the same binary interaction correlations proposed in this work were also used for the original SRK, PR, and PT equations. It is evident that for all the gases, the Z-factors calculated using the thermodynamic model proposed in this work had the best matches with the experiment data. The simulation results for the models based on the original SRK (Soave, 1972), PR (Peng and Robinson, 1976), and PT (Patel and Teja, 1982) EOSs and the Beggs (Beggs and Brill., 1973) and Ehsan (Ehsan et al., 2010) correlations showed the same change trend with a change in pressure as the experimental data. However, their modeling results deviated from the experimental data to different degrees, with the modeling results of the PT EOS relatively closer to the experimental data than the others, followed by the PR and SRK EOSs. The calculation results when using the Beggs (Beggs and Brill., 1973) and Ehsan (Ehsan et al., 2010) empirical correlations deviated from the experimental data to some degree, which became more obvious with an increase in the CO₂ content of the natural gas. This might have been due to the scarcity of available Z-factor experimental data for this kind of natural gas when building the correlations. At the same time, it meant that a thermodynamic model based on an EOS might be more suitable for describing the volumetric properties of natural gases.

Table 2 further provides the prediction deviations of these tested models. The absolute average deviation (AAD) of the model proposed in

Table 2

Prediction accuracies for compressibility factors of gas samples using four thermodynamic models and two empirical correlations.

Gas sample	Relative deviation, %					
	This work	SRK (Soave, 1972)	PR (Peng and Robinson, 1976)	PT (Patel and Teja, 1982)	Beggs (Beggs and Brill., 1973)	Ehsan (Ehsan et al., 2010)
sample 1	1.46	5.43	1.27	3.77	1.18	3.21
sample 2	0.34	4.20	1.52	2.83	1.02	2.92
sample 3	0.73	3.97	1.94	0.91	4.28	3.05
sample 4	0.50	4.16	1.50	2.56	3.04	2.39
sample 5	0.14	3.36	2.27	1.24	6.50	5.34
sample 6	0.25	2.99	2.77	0.72	8.19	9.30
sample 7	0.17	2.01	4.20	1.95	9.41	13.30
sample 8	0.46	2.85	3.53	1.66	13.82	17.68
TAD ^a , %	0.51	3.62	2.37	1.96	5.93	7.15

^a TAD: total average deviation.

this work was only 0.51%, which was much smaller than those of the models used for comparison. It should be noted that the thermodynamic models based on the original SRK, PR, and PT EOSs also showed high prediction accuracies, with the total average deviations between the simulation results and experimental data equal to 3.62%, 2.37%, and 1.96%, respectively. In agreement with the results shown in Fig. 6, the predicted deviations of the Beggs (Beggs and Brill, 1973) and Ehsan (Ehsan et al., 2010) correlations quickly increased with an increase in the CO₂ concentration of the natural gas. For example, when using these correlations for sample 8, the highest relative deviations between the experimental Z-factors and calculation results were 13.82% and 17.68%, respectively. In short, the test of the thermodynamic model developed in this work, in which the modified SRK EOS was combined with corrected interaction correlations between CH₄ or CO₂ and other gas components, showed that it might be suitable for describing the Z-factor of natural gas that contains CO₂, even at ultra-high temperatures and pressures.

Fig. 7 presents the P-T phase envelope curves of samples 1–8. As can be seen, the reservoir conditions of all the samples were located in the supercritical region. Because both the critical temperature and critical pressure of the CO₂ were higher than those of CH₄, the critical point of the natural gas gradually moved to the upper right with an increase in the CO₂ content of the natural gas. For sample 2, after CO₂ was injected at 50 mol% and 90 mol%, its critical temperature increased from the original 195.59 K–253.44 K and 296.52 K, respectively, with the critical pressure changing from the original 4.98 MPa–8.69 MPa and 7.94 MPa, respectively.

As stated above, to establish the thermodynamic model in this work, 165 Z-factor data points reported in the literature (Buxton, 1965) were used. Fig. 8 shows the relation between these reported experimental Z-factor values and the results calculated using the model proposed in this work. It was found the TAD between the experimental data and calculated values was still only 0.78%.

To further validate the model proposed in this work for calculating natural gas Z-factors, Z-factor calculations were performed for some other natural gases reported in the literature (Hou et al., 1996; Fayazi et al., 2014; Li and Guo, 1991; Bian et al., 2012; Sarem, 1961; Mcleod, 1968) that were not employed during the model development process in this work. The comparison results are shown in Fig. 9. For these cited data (418 points), the temperature range was 263.15–344.26 K, pressure range was 0.11–48.46 MPa, and CO₂ concentration range was 0–50.99 mol%. It was observed that the calculated Z-factors still fit well with the reported experimental data. It is important to note that for these reported 418 Z-factor points, the TAD between the experimental data and results calculated using the model proposed in this work was still only

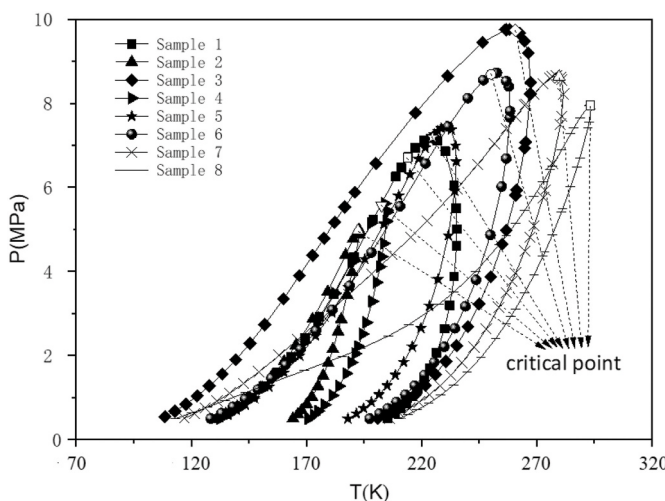


Fig. 7. Phase envelope curves of considered gas samples.

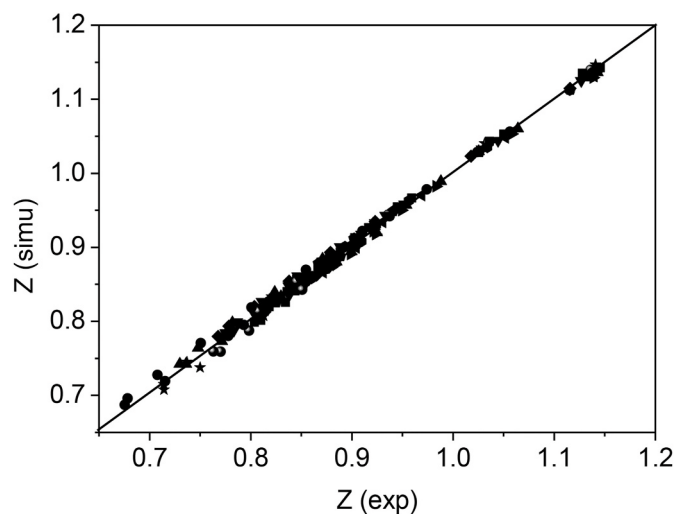


Fig. 8. Comparison of Z-factors reported in literature (Buxton, 1965) (Z-exp) and values (Z-simu) calculated in this work, where these reported Z-factors were used to build the thermodynamic model proposed in this work.

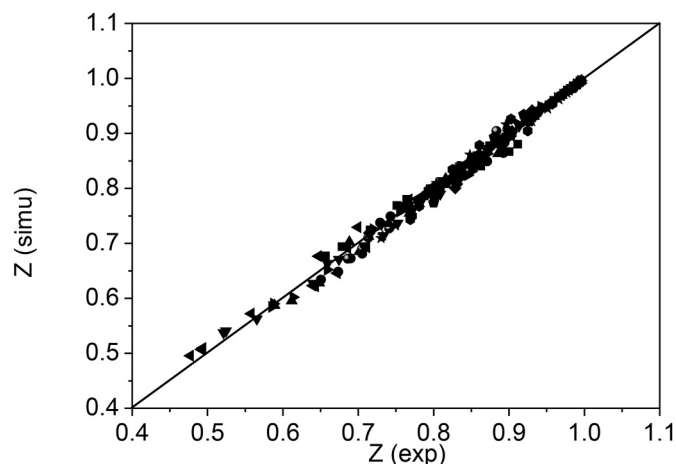


Fig. 9. Comparisons of some experimental Z-factors from literatures (Hou et al., 1996; Fayazi et al., 2014; Li and Guo, 1991; Bian et al., 2012; Mcleod, 1968) (Z-exp) with values (Z-simu) calculated using model proposed in this work.

0.93%, again demonstrating the wide applicability of the proposed model.

5. Conclusions

Two low-permeability gas reservoir natural gas samples (sample 1 and sample 2) and one ultra-high temperature ultra-high pressure high CO₂-containing gas reservoir natural gas sample (sample 3) were collected from real gas fields in China. Meanwhile, five artificial CO₂-natural gas mixtures were prepared in the laboratory by injecting different amounts of CO₂ into sample 2. The Z-factors of these eight gas samples were determined on the basis of constant composition expansion experiments. It was found that because the C₂–C₄ hydrocarbon concentrations in sample 1 were somewhat higher than those in sample 2, the Z-factors of sample 1 were somewhat smaller than those of sample 2. The injection of CO₂ into sample 2 substantially decreased the Z-factor. The ultra-high temperature and ultra-high pressure reservoir conditions caused sample 3 to show much higher Z-factors than sample 1 and sample 2, even though the former also had a much higher CO₂ concentration. A model based of the modified SRK EOS was further

proposed to predict the Z-factors of investigated gas mixtures, in which a new correlation for calculating the m parameter in the $a(T)$ function of the SRK EOS was built. The accuracy of the proposed model was verified by comparison with three other EOSs and four empirical correlations from the literature. It was demonstrated that the model developed in this work favored describing the Z-factors of natural gases with a wide range of CO₂ concentrations and reservoir temperature and pressure ranges. The research results obtained in this work should be beneficial for the development of low-permeability natural gas reservoirs using CO₂ flooding, as well as ultra-high pressure natural gas reservoirs containing high CO₂ levels.

Declaration of competing interest

The authors declare that they have no known competing financial interests or personal relationships that could have appeared to influence the work reported in this paper.

Acknowledgements

The financial support received from the National Major Project of China (No. 2016ZX05048003) and Sichuan Province Key Fund (No. 21QYCX0027), is gratefully acknowledged.

Nomenclatures

p	pressure
V	volume
T	temperature
Z	compressibility factor
R	the reduction ratio
k_{ij}	binary interaction parameters
T_r	relative temperature
T_c	critical temperature
P_c	critical pressure
ω	eccentricity factor
a	equation of state energy parameter
b	equation of state volume parameter
d	reduction ratio

Appendix A. Supplementary data

Supplementary data to this article can be found online at <https://doi.org/10.1016/j.jngse.2020.103759>.

References

- Beggs, D.H., Brill, J.P., 1973. A study of two-phase flow in inclined pipes. *J. Petrol. Technol.* 607–617.
- Bian, X., Du, Z., Tang, Y., et al., 2012. Measurement and correlation of compressibility factor of high CO₂-content natural gas. *J. Petrol. Sci. Eng.* 82–83, 38–43.
- Bowker, K.A., 2007. Barnett shale gas production, Fort Worth Basin: issues and discussion. *Am. Assoc. Petrol. Geol. Bull.* 91, 523–533.
- Buxton, T.S., 1965. The Prediction of the Compressibility Factor for Lean Natural Gas - Carbon Dioxide Mixtures at High Pressure, Doctor Thesis. The University of Oklahoma.
- Dou, H., Zhang, H., Yao, S., et al., 2016. Measurement and evaluation of the stress sensitivity in tight reservoirs. *Petrol. Explor. Dev.* 43, 1116–1123.
- Dria, D.E., Pope, G.A., Sepehrnoori, K., 1993. Three-phase gas/oil/brine relative permeabilities measured under CO₂ flooding conditions. *SPE Reservoir Eng.* 8, 143–150, 02.
- Ehsan, H., Amir, S., Jashid, M., 2010. A novel correlation approach for prediction of natural gas compressibility factor. *J. Nat. Gas Chem.* 19, 189–192.
- Fayazi, A., Arabloo, M., Mohammadi, A.H., 2014. Efficient estimation of natural gas compressibility factor using a rigorous method. *J. Nat. Gas Sci. Eng.* 16, 8–17.
- Guo, P., Liu, H., Wang, C., et al., 2020. The determination of phase behavior properties of high-temperature high-pressure and rich condensate gases. *Fuel* 280, 118568.
- Heidaryan, E., Moghadasi, J., Rahimi, M., 2010. New correlations to predict natural gas viscosity and compressibility factor. *J. Petrol. Sci. Eng.* 73, 67–72.
- Hou, H., Holste, J.C., Hall, K.R., 1996. Second and third virial coefficients for methane + ethane and methane + ethane + carbon dioxide at (300 and 320) K. *J. Chem. Eng. Data* 41, 344–353.
- Huron, M.J., Vidal, J., 1979. New mixing rules in simple equations of state for representing vapor-liquid equilibria of strongly non-ideal mixtures. *Fluid Phase Equilibil* 3, 255–271.
- Kamari, A., Hemmati-Sarapardeh, A., Mirabbasi, S.M., et al., Prediction of sour gas compressibility factor using an intelligent approach. *Fuel Process. Technol.* 116, 209–216.
- Kamyab, M., Sampaio Jr., J.H.B., Qanbari, F., et al., 2010. Using artificial neural networks to estimate the z-factor for natural hydrocarbon gases. *J. Petrol. Sci. Eng.* 73, 248–257.
- Katz, D.L.V., 1959. Handbook of Natural Gas Engineering[M]. McGRAW-HILL.
- Krooss, B.M., Van Bergen, F., Gensterblum, Y., et al., 2002. High-pressure methane and carbon dioxide adsorption on dry and moisture-equilibrated pennsylvanian coals. *Int. J. Coal Geol.* 51, 69–92.
- Kumar, N., 2004. Compressibility Factor for Natural and Sour Reservoir Gases by Correlations and Cubic Equations of State. Texas Tech University. M. Sc. (Thesis).
- Kumar, N., 2005. Compressibility Factor for Natural and Sour Reservoir Gases by Correlations and Cubic Equations of State, MS Thesis. Texas Tech University, Lubbock, Tec, USA.
- Li, Q., Guo, T.M., 1991. A study on the supercompressibility and compressibility factors of natural gas mixtures. *J. Petrol. Sci. Eng.* 6, 235–247.
- Liu, H., Wu, Y., Guo, P., et al., 2019. Compressibility factor measurement and simulation of five high-temperature ultra-high-pressure dry and wet gases. *Fluid Phase Equil.* 500, 112256.
- Mamora, D.D., Seo, J.G., 2002. Enhanced gas recovery by carbon dioxide sequestration in depleted gas reservoirs. In: SPE Annual Technical Conference and Exhibition, 29 September–2 October, San Antonio, Texas.
- McLeod, W.R., 1968. Applications of Molecular Refraction of the Principle of Corresponding States, Doctor Thesis. The University of Oklahoma.
- Mohasen-Nia, M., Moddareddi, H., Mansoori, G.A., 1994. Sour natural gas and liquid equation of state. *J. Petrol. Sci. Eng.* 12, 127–136.
- Patel, N.C., Teja, A.S., 1982. A new cubic equation of state for fluids and fluid mixtures. *Chem. Eng. Sci.* 37, 463–473.
- Peng, D.Y., Robinson, D.B., 1976. A new two constant equation of state. *Ind. Eng. Chem. Fundam.* 15, 59–64.
- Sanjan, E., Lay, E.N., 2012. Estimation of natural gas compressibility factors using artificial neural network approach. *J. Nat. Gas Sci. Eng.* 9, 220–226.
- Sanjari, E., Lay, E., 2012. An accurate empirical correlation for predicting natural gas compressibility factors. *J. Nat. Gas Chem.* 21, 184–188.
- Sanjari, A., Nemati Lay, E., 2012. Estimation of natural gas compressibility factors using artificial neural network approach. *J. Nat. Gas Eng.* 9, 220–226.
- Sarem, A.M., 1961. Z-factor equation developed for use in digital computers. *Oil Gas J.* 118.
- Shi, Y., Jia, Y., Pan, W., et al., 2017. Mechanism of supercritical CO₂ flooding in low-permeability tight gas reservoirs. *Oil Gas Geol.* 38, 610–616 (In Chinese).
- Soave, G., 1972. Equilibrium constants from a modified Redlich-Kwong equation of state. *Chem. Eng. Sci.* 27, 1197–1203.
- Strvjejk, R., Vera, J.H., 1986. PRSV: an improved Peng-Robinson equation of state for pure compounds and mixtures. *Can. J. Chem. Eng.* 64, 323–333.
- Wang, X., Economides, M., 2009. Advance Natural Gas Engineering. Gulf Publishing Company, Houston, Texas.
- Wei, L., Lu, X., Song, Y., 2009. Formation and pool-forming model of CO₂ gas pool in eastern Changde area, Songliao Basin. *Petrol. Explor. Dev.* 36, 174–180.
- Xiao, Y., Yan, K., Wang, H., et al., 2012. Sun. A new approach to predicting the compressibility factor of ultra high-pressure gas reservoirs. *Nat. Gas. Ind.* 32, 42–46.
- Yan, K.L., Liu, H., Sun, C.Y., et al., 2013. Measurement and calculation of gas compressibility factor for condensate gas and natural gas under pressure up to 116 MPa. *J. Chem. Thermodyn.* 63, 38–43.
- Yin, S., Ding, W., Zhou, W., et al., 2017. In situ stress field evaluation of deep marine tight sandstone oil reservoir: a case study of Silurian strata in northern Tarim Basin, NW China. *Mar. Petrol. Geol.* 80, 49–69.
- Zeng, J., Zhang, Y., Zhang, S., et al., 2016. Experimental and theoretical characterization of the natural gas migration and accumulation mechanism in low-permeability (tight) sandstone cores. *J. Nat. Gas Sci. Eng.* 33, 1308–1315.
- Zhang, F., Li, J., Wei, G., et al., 2018. Formation mechanism of tight sandstone gas in areas of low hydrocarbon generation intensity: a case study of the Upper Paleozoic in north Tianhuan depression in Ordos Basin, NW China. *Petrol. Explor. Dev.* 45, 79–87.
- Zou, C., Zhu, R., Liu, K., et al., 2012. Tight gas sandstone reservoirs in China: characteristics and recognition criteria. *J. Petrol. Sci. Eng.* 88–89, 82–91.